The Linnean Society of London BIOLOGICAL Journal of the Linnean Society

Biological Journal of the Linnean Society, 2010, **99**, 99–117. With 11 figures

Evolution of ontogenetic allometry shaping giant species: a case study from the damselfish genus *Dascyllus* (Pomacentridae)

BRUNO FRÉDÉRICH[1]* and H. DAVID SHEETS[2]

[1]*Laboratoire de Morphologie fonctionnelle et évolutive, Institut de Chimie (B6c), Université de Liège, B-4000 Liège, Belgique*
[2]*Department of Physics, Canisius College, 2001 Main Street, Buffalo, NY 14208, USA*

Received 6 March 2009; accepted for publication 2 July 2009

The evolution of body size, the paired phenomena of giantism and dwarfism, has long been studied by biologists and paleontologists. However, detailed investigations devoted to the study of the evolution of ontogenetic patterns shaping giant species are scarce. The damselfishes of the genus *Dascyllus* appear as an excellent model for such a study. Their well understood phylogeny reveals that large-bodied species have evolved in two different clades. Geometric morphometric methods were used to compare the ontogenetic trajectories of the neurocranium and the mandible in both small-bodied (*Dascyllus aruanus* and *Dascyllus carneus*; maximum size: 50–65 mm standard length) and giant (*Dascyllus trimaculatus* and *Dascyllus flavicaudus*; maximum size: 90–110 mm standard length) *Dascyllus* species. At their respective maximum body size, the neurocranium of the giant species is significantly shorter and have a higher supraoccipital crest relative to the small-bodied species, whereas mandible shape variation is more limited and is not related to the 'giant' trait. The hypothesis of ontogenetic scaling whereby the giant species evolved by extending the allometric trajectory of the small-bodied ones (i.e. hypermorphosis) is rejected. Instead, the allometric trajectories vary among species by lateral transpositions. The rate of shape changes and the type of lateral transposition also differ according to the skeletal unit among *Dascyllus* species. Differences seen between the two giant species in the present study demonstrate that giant species may appear by varied alterations of the ancestor allometric pattern. *Biological Journal of the Linnean Society*, 2010, **99**, 99–117.

ADDITIONAL KEYWORDS: coral reef fishes – development – geometric morphometrics – giantism – growth – heterochrony – trajectory – shape – size – skull.

INTRODUCTION

Evolutionary change in body size is one of the most common patterns in the history of life (LaBarbera, 1989; Shea, 1992). Change in body size within an evolutionary lineage over time has been studied subsequent to the synthesis of Cope's rule stating the tendency for organisms to evolve larger bodies (Hone & Benton, 2005). An increase in body size is considered to convey many advantages (e.g. mating success, defense against predation, easier access to valuable food sources) on an organism but also carries disadvantages (e.g. longer development time, higher food requirements) (Forsman & Lindell, 1993; Benton, 2002; Hone & Benton, 2005). The evolution of changes in body size may be observed at different taxonomic levels (Hone *et al.*, 2008). However, highly detailed studies of shape changes associated with body size evolution, particularly those seeking to go beyond the simple categories of paedomorphism and peramorphism by considering a wider range of processes, have been limited in number. In the present study, we sought to extend the study of evolution of body size by examining at the ontogenetic patterns associated with changes in body size.

The Pomacentridae (damselfishes) is one of the most conspicuous fish families of the coral reef ecosystems (Allen, 1991). The genus *Dascyllus* comprises

*Corresponding author. E-mail: bruno.frederich@ulg.ac.be

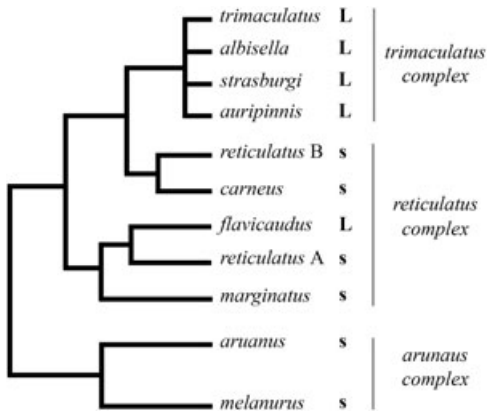

Figure 1. Phylogenetic relationships among the *Dascyllus* species. The topology is based on data presented by McCafferty *et al.* (2002). L and s were, respectively, assigned to the large-bodied and small-bodied species. *Dascyllus reticulatus A* and *B* refer to distinct populations living, respectively, in the northern western Pacific and the southern western Pacific.

ten species found throughout the tropical region of the Indo-West Pacific (Randall & Allen, 1977; Randall & Randall, 2001). Their phylogenetic relationships are now well understood (Fig. 1) (Godwin, 1995; Bernardi & Crane, 1999; McCafferty *et al.*, 2002) and all species have been grouped into three species complexes on the basis of morphology, biogeography and striking coloration differences: the *Dascyllus aruanus*, *Dascyllus reticulatus*, and *Dascyllus trimaculatus* complexes (Fig. 1) (Godwin, 1995). All species are primarily planktivorous (Randall & Allen, 1977). The members of the *D. aruanus* (*D. aruanus* [L.] and *Dascyllus melanurus* [Bleeker]) and *D. reticulatus* (*D. reticulatus* [Richardson], *Dascyllus carneus* Fischer, *Dascyllus marginatus* [Rüppell], and *Dascyllus flavicaudus* Randall & Allen) complexes are small-bodied with a maximum standard length (SL = length from the tip of the snout to the posterior edge of the caudal peduncle) of 50–65 mm, except *D. flavicaudus* which is a large-bodied species reaching a maximum SL of 90 mm (Randall & Allen, 1977). These six species live in social groups strongly associated with branched corals (acroporan, pocilloporan, and stylophoran corals) where they seek shelter at night or when danger threatens during the day. This association with coral heads is an obligate relationship throughout life for the smaller species (Sale, 1971), but not for the large-bodied *D. flavicaudus* (Godwin, 1995). Their social groups are highly size-structured where small fish are always subordinate to larger ones (Coates, 1980). The members of the *D. trimaculatus* complex (*D. trimaculatus* [Rüppell], *Dascyllus albisella* Gill, *Dascyllus strasburgi* Klausevitz, and *Dascyllus auripinnis* Randall & Randall) are large-bodied fish with a maximum SL of 90–110 mm (Randall & Allen, 1977). Juveniles of these four species are closely associated with heads of coral or with sea anemones, whereas adults form large feeding groups over the reef. This ontogenetic shift in habitat occurs at the sexual maturity which is size related (approximately 70 mm SL) (Booth, 1995).

The phylogenetic data show that the ancestral *Dascyllus* was small-bodied and that large-bodied (giant) species have evolved in two clades: the *D. trimaculatus* and the *D. reticulatus* complexes (Fig. 1). The giant species almost doubled in size compared to the small ones. The ecological and/or ethological processes leading to the emergence of these giant species remain unknown (Godwin, 1995). Through its evolution, the genus *Dascyllus* appears as an excellent model for the study of evolutionary modifications in ontogenetic allometries shaping giant species.

Allometry refers to the pattern of covariation among morphological traits or between measures of size and shape (Klingenberg, 1998). Procrustes based geometric morphometrics are grounded on a separation of size and shape and are thus a useful tool for studying allometry (Zelditch *et al.*, 2004). Geometric morphometric studies of the ontogeny of animal taxa are numerous (Monteiro, Cavalcanti & Sommer, 1997; Zelditch, Sheets & Fink, 2000; Bastir & Rosas, 2004; Cardini & O'Higgins, 2005; Ivanović *et al.*, 2007) and mainly report divergent trajectories among species in the size-shape space. Using an analysis based on the finite-element scaling method (for methodology, see Cheverud *et al.*, 1983), Corner & Shea (1995) compared the allometric patterns between giant transgenic mice and a control population. They concluded that the form differences between control and transgenic adults predominantly result from ontogenetic scaling (i.e. an extension of the ancestral allometric trajectory). To our knowledge, other studies specifically devoted to the study of the evolution of allometric patterns shaping giant (or dwarf) species remains limited (Weston, 2003; Hunda & Hughes, 2007; Marroig, 2007). Interpreted in terms of heterochronic changes, the *Dascyllus* lineage could exemplify a case of proportioned giantism or hypermorphosis. However, the conservation of an ontogenetic trajectory in both the ancestor (small-bodied species) and descendant (large-bodied species) that is required to satisfy a testable definition of heterochrony has yet to be demonstrated (Webster & Zelditch, 2005).

In the present study, we aim to compare the ontogenetic allometry of the neurocranium and the mandible within the genus *Dascyllus*. In this examination of the evolution of giantism, we address the following questions:

1. Do the large-bodied species share the same allometric trajectories of the small-ones, or is there evidence of allometric repatterning during development?
2. Knowing that shape differences might be expected as a result of diverse functional constraints related to size, do the large-bodied species differ in shape from the small ones at the adult stage?
3. Does the dynamics of shape change differ between *Dascyllus* species? Are these rate modifications (rate heterochrony) or allometric repatterning? Or have changes in shape already appeared during an earlier period of the development?
4. Along the same size range, does the amount of shape change differ between *Dascyllus* species? (coupled with an absence of allometric repatterning, this would be clear evidence of heterochronic changes)
5. Knowing that large-bodied *Dascyllus* species have evolved in two clades (Fig. 1), does the pattern of allometry evolve similarly in large-bodied species belonging to these two different lineages?

MATERIAL AND METHODS

Samples

A total of 231 specimens belonging to four species of the genus *Dascyllus* and two of the genus *Chromis* were analysed (Table 1). *Dascyllus trimaculatus* and *D. flavicaudus* were the large-bodied species studied, whereas *D. aruanus* and *D. carneus* represented the small-bodied species. Ontogenetic series were drawn from natural populations of one or two close geographical regions (Table 1), except for *D. trimaculatus*, in which the series is made up of specimens coming from Toliara (Madagascar) and Moorea (Society Islands, French Polynesia). No information is available on possible geographic variations in skeletal morphology but *D. trimaculatus* have the same life cycle and habitat in Madagascar and French Polynesia (Randall & Allen, 1977). Consequently, a hypothetical influence of geographical variation should be very limited on its ontogenetic pattern. Two *Chromis* species were used as an outgroup for comparing ontogenies (Zelditch *et al.*, 2000), *Chromis viridis* ($N = 15$) and *Chromis atripectoralis* ($N = 21$). These two very close species are named the blue green damselfishes, differing only by the coloration of the pectoral fin base (Froukh & Kochzius, 2008). The allometric trajectories of these two species did not differ significantly [analysis of covariance (ANCOVA) revealed no differences in the linear regressions of body size versus structure size (i.e. centroïde size), see below] between the two species ($P < 0.05$). Consequently, the samples of the two species were pooled to build a single estimated ontogeny of the outgroup referred as *Chromis* sp. along this study. Some *D. carneus* specimens come from the collections the Academy of Natural Sciences (Philadelphia, PA, USA), the National Museum of Natural History (Washington, DC, USA) and the Museum National d'Histoire Naturelle (Paris, France). Detailed information on specimen catalog numbers is available in the Appendix. The others were collected in the lagoon or on the outer reef slope at Toliara (Mozambique Channel, Madagascar) in June 2004, October 2006, and November 2007; and at Moorea (Society Islands, French Polynesia) in June 2007 after being anaesthetized by a solution of quinaldine. Fishes were preserved in neutralized and buffered 10% formalin for 10 days, then transferred to 70% alcohol. All specimens were cleared and stained with alizarin red S (Taylor & Van Dyke, 1985) to display the osseous skeleton.

Morphometric methods

To examine the allometric patterns, we use landmark-based geometric morphometric methods (Bookstein, 1991, Rohlf & Marcus, 1993; Adams, Rohlf & Slice, 2004). Sixteen homologous landmarks (LM) were defined on lateral views of the neurocranium and 12 on the mandible (Fig. 2), forming two separate data sets. All landmarks are described in Frédérich *et al.* (2008a). Several steps were taken to reduce measurement errors: (1) each structure is positioned in glass pearls so to stabilize them in a comparable lateral plane; (2) each structure is sufficiently laterally flattened, so the projection of three-dimensional landmarks into a two-dimensional plane involves a low

Table 1. Studied species with sample size

Species	Abbreviations	Geographical area	SL^{max}	SL^{mm}	N_{neuro}	N_{man}
Chromis sp.		French Polynesia	70	7–77	33	35
Dascyllus aruanus	*D. aru*	Madagascar	50–65	10–60	49	49
Dascyllus carneus	*D. car*	Madagascar and Seychelles Islands	50–65	17–67	45	46
Dascyllus flavicaudus	*D. fla*	French Polynesia	90	17–74	40	42
Dascyllus trimaculatus	*D. tri*	Madagascar and French Polynesia	90–110	10–100	54	59

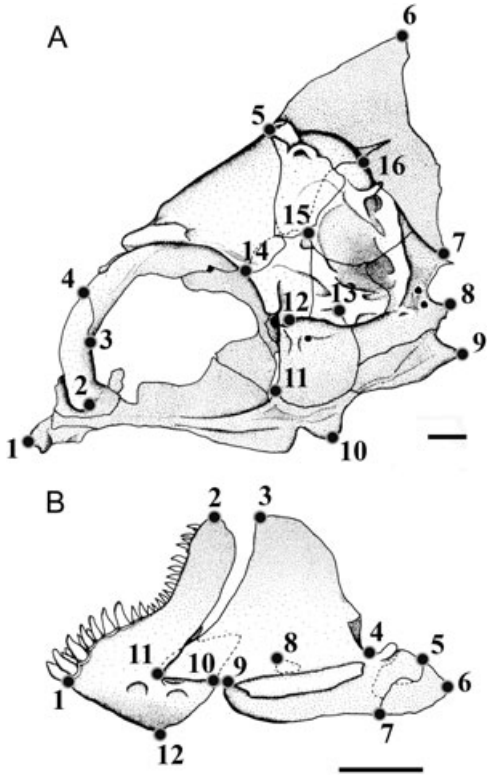

Figure 2. Landmarks used in the present study on (A) the neurocranium and (B) the mandible. Scale bars = 1 mm.

dimensionality reduction error. All measurements were made by the same person (BF) in the four *Dascyllus* species and in *Chromis* sp. using a Leica M10 binocular microscope coupled to a camera lucida. Lucida images drawn on sheets were then scanned and the x and y coordinates of landmarks were digitized using TPSDIG, version 1.40. As shown in Table 1, the size of samples differed slightly between the two structures because some skulls were damaged before or during the dissection.

A generalized procrustes analysis was performed for each structure aiming to superimpose all specimens in a way that removes differences as a result of translation, rotation and scale (Rohlf & Slice, 1990; Zelditch *et al.*, 2004). The grand mean (i.e. the consensus of all specimens) was calculated and shape variables were then generated as partial warp scores (PWs) including both uniform and non-uniform components (Bookstein, 1991; Rohlf, 1993). Thin plate spline functions (Bookstein, 1991) and plots of landmark displacements are used to depict results of ordinations and regression models. The centroid size (CS) of the structure was also computed as the square root of the sum of the squares of the distances from all LMs to their centroid (Bookstein, 1991). Age information is not available for our specimens, and so all analyses must rely on size as a proxy for age.

Visual exploration of ontogenetic trajectories using principal component analysis (PCA) of shape data, and of size and shape (Procrustes form space or size-shape space; Mitteroecker *et al.*, 2004; Mitteroecker, Gunz & Bookstein, 2005) of the PWs plus the natural log of the centroid size (ln-CS) were examined. *Chromis* sp. was first included in the PCA aiming to determine whether the allometric patterns differ between *Chromis* sp. and the *Dascyllus* species. Then, the analyses were repeated after excluding this species to observe variations in allometric models within *Dascyllus* species.

However, the descriptions of ontogenetic trajectories in the shape space defined by the first principal components, although informative, may be misleading (Mitteroecker *et al.*, 2004, 2005) because it is often difficult to assign the first PC axis to a specific biological cause, as also noted by Angielczyk & Sheets (2007) when attempting to isolate ontogenetic signals from other sources of variance. Mitteroecker *et al.* (2004, 2005) particularly emphasize that PCA is an exploratory technique, which we would like to bolster with statistical approaches to hypothesis testing. Consequently, the allometric patterns of shape variation were also analysed using linear multivariate regression of PWs on log-transformed size (ln-CS) (Monteiro, 1999; Zelditch *et al.*, 2004; Mitteroecker *et al.*, 2005; Frédérich *et al.*, 2008b). Plots of procrustes distance from the juvenile form, and the variance explained by the models are used to assess the validity of log-linear models. The null hypothesis that shape develops isometrically was tested in all species using TPSREGR, version 1.34. The fit of the regression models was evaluated by the explained variance of the model and by a permutation test based on a generalized Goodall's F-test with 10 000 permutations.

Differences in allometric trajectories among species were tested by a full multivariate analysis of covariance (MANCOVA), testing the null hypothesis of homogeneity of linear allometric models. In these tests for common slopes and homogeneity of intercepts, shape variables (PWs) are considered as dependent variables, size (ln-CS) as covariate, and species are grouping factor. *Chromis* sp. was first included in the comparison of allometric trajectories of species. Then, the MANCOVA was repeated after excluding this species to test variations in allometric models within *Dascyllus* species. If the MANCOVA establishes strong evidence of differences in ontogenies, other tests will be used to establish the nature of the differences.

As suggested by Zelditch *et al.* (2000) and Webster & Zelditch (2005), two factors can explain differences in allometric models: (1) the divergence of allometric

trajectories (allometric repatterning) and (2) the rate of shape changes (which could be interpreted as heterochrony if the directions of the ontogenetic vectors are the same). Consequently, we estimated and compared both factors when the allometric models differed. The differences in trajectories of shape changes were analysed by comparing the angle between the species-specific multivariate regression vectors using VECCOMPARE6 (IMP Software). This test is described in detail elesewhere (Zelditch *et al.*, 2000, 2004). Briefly, in the context of the present study, a within-species vector is composed of all regression coefficients of the shape variables (PWs) and the log-transformed CS. The range of angles between such vectors within each species is calculated using a bootstrapping procedure ($N = 400$). This range was than compared with the angle between the vectors of both species. If the between-species angle exceeds the 95% range of the bootstrapped within-species angles, the between-species angle is considered significantly different, and thus the allometric trajectories are different. The allometric vector of all *Dascyllus* species and *Chromis* sp. was compared species by species.

We also use a cross-validation procedure to determine whether two or more species share a common direction to their ontogenetic trajectory, but differ in rate along that direction or whether they are better described as having different directions of the trajectories. We begin by considering regression models for the dependence of shape ($\boldsymbol{Y}$) on our size variable (log centroid size, x in this case) of the form:

$$\boldsymbol{Y} = \boldsymbol{M}_{\mathrm{i}} x + \boldsymbol{B}_{\mathrm{i}} + \boldsymbol{\varepsilon} \quad (1)$$

where $\boldsymbol{M}_{\mathrm{i}}$ is the multivariate slope (or ontogenetic growth vector) of the ith species, and $\boldsymbol{B}_{\mathrm{i}}$ is the intercept value, and ε is a matrix of residuals, representing the unexplained variance in the model (bold denotes a multivariate variable, i.e. a vector quantity). Standard MANCOVA methods will allow us to determine if the slopes $\boldsymbol{M}_{\mathrm{i}}$ and intercepts $\boldsymbol{B}_{\mathrm{i}}$ differ among the different groups (typically species for our purposes) in the study. If the slopes and intercepts differ among the species in a statistically significant manner, we are left with several possibilities as to how the slopes ($\boldsymbol{M}_{\mathrm{i}}$) differ. In particular, we would like to test the hypothesis that the species in question share a common direction $\boldsymbol{M}_{\mathrm{c}}$ of ontogenetic trajectory, differing only in a relative rate of growth along that trajectory, which we might call a_{i}, a species-specific relative rate along the trajectory, thus being a simpler model than Eqn (1), which has independent vector slopes for each species. This results in a regression model of the form:

$$\boldsymbol{Y} = \boldsymbol{M}_{\mathrm{c}} \alpha_{\mathrm{i}} x + \boldsymbol{B}_{\mathrm{i}} + \boldsymbol{\varepsilon} \quad (2)$$

It is possible to fit Eqn (1) to observed multivariate data, using standard regression modelling to estimate the parameters $\boldsymbol{M}_{\mathrm{i}}$, $\boldsymbol{B}_{\mathrm{i}}$ for each of the species (i) in the study. To fit Eqn (2), however, we used numerical optimization methods (a downhill simplex search; Press *et al.*, 2007) to determine the parameter values because an analytic method was not readily available. In both cases, the parameters are chosen so as to minimize the summed squared errors, represented by ε in Eqns 1 and 2. Because Eqn (1) has more parameters than Eqn (2), we expect that the fitting error (summed square residuals) of Eqn (1) will always be less than or equal to the fitting error of Eqn (2) because Eqn (2) has fewer parameters, and is a simplified, 'nested' version of Eqn (1). So, even in the case where Eqn (2) is 'correct', Eqn (1) should produce lower fitting errors.

If we had a maximum likelihood model available that described the distribution of the errors (ε), it would be possible to compare the models using a log-likelihood ratio test, or the Aikake Information Criteria approach. However, for the landmark-based shape data used in the present study, maximum likelihood models do not appear to be available. The alternative approach taken here is to use cross-validation methods to estimate the performance of the models on test data. In cross-validation, some portion p (typically 1–50%) of the data is separated out to form a test set, and the model is then fitted to the remaining fraction $(1 - p)$ of the data, which is referred to as a learning or fitting set. The model is then used to predict the measurements Y of the test data set, which allows calculation of a cross-validation error, the summed squared residuals from the model of the data in the test set. This cross-validation error is a better estimate of how the model would perform with new data than the fitting error discussed earlier. This cross-validation procedure may be repeated many times, randomly dividing the data into the test and learning sets each time, to estimate the distributions of the cross-validation error associated with each model.

Under ideal circumstances, the 'true' model will produce consistently lower rates of cross-validation error. Models which are too simple will fail to explain as much variance in the data as the 'true' model, whereas models which are too complex will 'overfit' the data, and thus produce higher levels of cross-validation error, although very large data sets may be necessary to detect overfitting. If large amounts of data are available, and one model is much closer to 'truth' than the other, cross-validation may detect it. It is possible to require that one model produce lower cross-validation error 95% of the time to reject the other model as inferior at a 5% level of confidence using this approach.

Additionally, we also explored the shape differences between the *Dascyllus* species at different sizes, par-

ticularly at their maximum size (SL_{Max}), in order to determine how the small-bodied and the large-ones vary in shape at various sizes. A standardized regression residual analysis was used (Zelditch, Sheets & Fink, 2003; Bastir & Rosas, 2004, noting the issues raised by Darlington & Smulders, 2001). From the multivariate regression of shape on ln-CS, the non-allometric residual fraction is standardized by STANDARD6 (IMP Software). 'Standardized' data sets of adults with their respective SL_{Max} (60 mm in *D. aruanus* and *D. carneus*; 90 mm in *D. flavicaudus*; 100 mm in *D. trimaculatus*), which are the predicted shapes of the entire population at these size, are generated. 'Standardized' data sets of specimens at two other sizes, 20 mm (juvenile) and 60 mm SL (an intermediate stage for giant species), were also generated. To assess the shape variation among *Dascyllus* at every size, canonical variate analyses (CVA) with a leave-one-out cross-validation assignment test were carried out using CVAGEN (IMP Software). Thin plate spline functions were used to display the shape features associated with the canonical variates (CVs). Additionally, at the three sizes, the amount of the overall shape differences between species was estimated using Procrustes distance (PD, calculated in the IMP software TWOGROUP), the metric defining shape dissimilarity in the Kendall shape space (Bookstein, 1996). The phenetic relationships were summarized with a cluster analysis calculated using both an unweighted pair group method with arithmetic mean (UPGMA) algorithm and nonmetric multidimensional scaling (NMMD). Permutation methods were performed using TwoGroup6 to test the null hypothesis of no mean difference between species at each size.

The rate of change in shape relative to size was also compared among *Dascyllus* species. Dynamics of shape changes were evaluated by calculating the PD between each specimen and the average shape of a the four smallest specimens in the datasets for each species. By regressing that distance on log-transformed CS, the rates of divergence away from the average juvenile shape were compared using the slope of the regressions with REGRESS6 (IMP Software); detailed explanations on this methodology are provided elsewhere (Zelditch *et al.*, 2003, 2004). Because the relationship between PD and ln-CS is close to linear, these can be statistically compared by ANCOVA.

Finally, we have also compared the amplitude of shape transformation observed during growth. TWOGROUP6 was used to calculate the PD between the average shapes of juveniles (20 mm SL) and adults with a maximum SL, and to test the statistical significance of the differences (resampling-based *F*-test). Bootstrapping procedures ($N = 400$) also permit: (1) placing confidence limits on this measure and (2) testing whether this measure of dissimilarity of shapes is significantly different among species.

Geometric morphometric analyses were performed using computer software from the TPS series (TPSDIG, TPSREGR, and TPSRELW), written by F. J. Rohlf (http://life.bio.sunysb.edu/morph/) and the IMP series (CVAGEN, REGRESS6, STANDARD6, VECCOMPARE, VECLAND, and TWOGROUP6), created by H. D. Sheets (available at: http://www2.canisius.edu/~sheets/morphsoft.html). TPS deformation grids were generated in MORPHEUS (Slice, 1999; http://life.bio.sunysb.edu/morph/morpheus/). STATISTICA, version 7.1 (Statsoft), was used for the statistical analysis (ANCOVA, MANCOVA, UPGMA). NNMDs and the cross-validated procedure were performed using MATLAB (The MathWorks).

RESULTS

Variation in allometric patterns

The PCAs indicate that the ontogenetic trajectories of the *Dascyllus* species strongly diverge from that of *Chromis* sp. in both Procrustes shape and form spaces. Ontogenetic shape variations in each *Dascyllus* and *Chromis* sp. species were summarized in Figure 3 by scatterplots of the PCA in Procrustes form space. When all species are combined (Fig. 3A, D), PC1, respectively, explains 97.7% and 91.5% of the variance in size and shape for the neurocranium and the mandible and PC2 explains 0.7% and 6.7%, respectively. The plots suggested that the shape differences between the small-bodied and the large-bodied *Dascyllus* species appear to be greater in the neurocranium than in the mandible at the maximum size. Differences in the ontogenetic trajectories among *Dascyllus* species (Fig. 3) were emphasized by the repetition of the PCA after excluding *Chromis* sp. For the neurocranium, PC3 represents differences between *D. flavicaudus* and the three other *Dascyllus* species (Fig. 3C). In this form space, the ontogenetic trajectory of *D. flavicaudus* is parallel to the shared trajectory by the three other species. Similar results were obtained in the mandible form space where the ontogenetic trajectory of *D. trimaculatus* is lateral transposed relative to the three other species (Fig. 3E, F). The ontogenetic trajectories shown for the neurocranium appear to be approximately linear, whereas trajectories in the mandible appear to be curved. However, it is worth noting that the second PC axis explains only 1.3% of the variance in the mandible compared to 97% for PC 1, so that a linear model of the trajectory as a function of log size is a reasonable approximation, given the small variance contained in the curving portion of the trajectory.

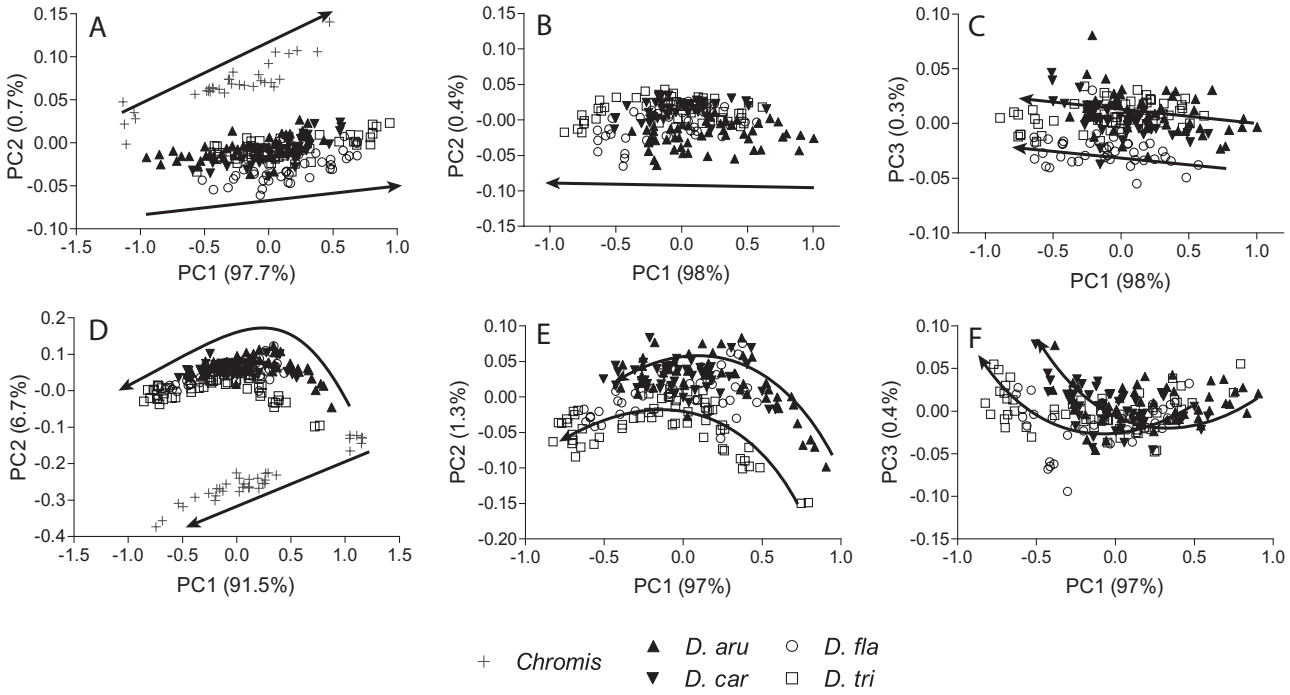

Figure 3. Principal components analyses illustrating ontogenetic trajectories for *Chromis* sp. and the five *Dascyllus* species in the Procrustes form shape space of (A–C) the neurocranium and (D–F) the mandible. Plots of the first three principal components (PC); percentage of shape variance summarized by each PC is given in parentheses. Arrows are added to depict the respective growth trajectories.

Table 2. Fit of regressions of shape versus log-values of centroid size (CS) for each structural unit

	Neurocranium % explained variance	Goodall's *F*-test		Mandible % explained variance	Goodall's *F*-test	
		F-value	*P*		*F*-value	*P*
Chromis sp	69.4	70.2620	0.0000	57.2	44.1881	0.0000
D. aru	41.6	33.4631	0.0000	70.6	113.5810	0.0000
D. car	35.1	23.2310	0.0000	60.2	66.7467	0.0000
D. fla	42.5	28.0689	0.0000	49.5	39.3018	0.0000
D. tri	68.7	114.1700	0.0000	72.1	148.6576	0.0000

For abbreviations of the species, see Table 1.

The null hypothesis of isometric growth is rejected for the five species as shape variation in the neurocranium and the mandible is significantly correlated with ln-CS (all *P* levels of the generalized Goodall's *F*-test < 0.05; Table 2). Allometry accounted for a large proportion (up to 72%) of total shape change during *Chromis* sp. and *Dascyllus* growth. The neurocranium showed a lower percentage of variance explained than the mandible (Table 2).

The full MANCOVA revealed significant interspecific differences in allometric models of the neurocranium and the mandible when *Chromis* sp. and every *Dascyllus* species were included in the analysis (test of common slopes: neurocranium, $\lambda_{Wilks} = 0.098$, $F = 5.212$, d.f. = 112, 733.4, $P < 0.001$; mandible, $\lambda_{Wilks} = 0.164$, $F = 5.804$, d.f. = 80, 799.3, $P < 0.001$; homogeneity of intercepts: neurocranium, $\lambda_{Wilks} = 0.005$, $F = 18.750$, d.f. = 112, 749.2, $P < 0.001$; mandible, $\lambda_{Wilks} = 0.003$, $F = 35.802$, d.f. = 80, 815.1, $P < 0.001$). After excluding *Chromis* sp., both tests indicated significant differences in allometric models within *Dascyllus* species (test of common slopes: neurocranium, $\lambda_{Wilks} = 0.307$, $F = 2.639$, d.f. = 84, 458.6, $P < 0.001$; mandible, $\lambda_{Wilks} = 0.463$, $F = 2.479$, d.f. = 60, 505, $P < 0.001$; homogeneity of intercepts: neurocranium, $\lambda_{Wilks} = 0.023$, $F = 13.809$, d.f. = 84, 467.5, $P < 0.001$;

Table 3. Angles in decimal degrees between the ontogenetic vector of *Chromis* sp and the four *Dascyllus*

		Neurocranium				Mandible			
Sp1	*Sp2*	Between	*Sp1*	*Sp2*	Difference	Between	*Sp1*	*Sp2*	Difference
Chromis	*D. aru*	40.0	12.6	21.5	S	20.6	15.9	10.7	S
	D. car	43.5	12.6	25.5	S	30.9	15.9	13.5	S
	D. fla	40.3	12.6	22.0	S	26.5	15.9	18.9	S
	D. tri	33.9	12.6	12.2	S	25.5	15.9	9.8	S
D. aru	*D. car*	20.2	19.9	22.4	NS	18.5	9.8	12.9	S
	D. fla	26.4	21.6	21.3	S	13.8	9.8	18.2	NS
	D. tri	20.7	19.9	10.7	S	9.5	9.1	9.6	NS
D. car	*D. fla*	23.2	22.9	20.7	S	18.1	12.6	17.2	S
	D. tri	23.0	22.6	10.5	S	14.1	12.8	9.1	S
D. fla	*D. tri*	20.4	22.6	11.4	NS	13.9	17.8	9.4	NS

Results are obtained by bootstrapping procedure ($N = 400$); the angle between ontogenetic vectors is considered significant if exceeds the bootstrapped within-group variance at 95% confidence: S, significant, NS, not significant. For abbreviations of the species, see Table 1.

mandible, $\lambda_{Wilks} = 0.049$, $F = 14.967$, d.f. = 60, 514, $P < 0.001$).

The analysis of the angles between multivariate regression vectors of ontogenetic allometries within- and between-species showed that, for both skeletal units, the angles between the four *Dascyllus* species and *Chromis* sp. were always higher than the ranges of the within-species angles (Table 3). Thus, all *Dascyllus* differ significantly in their ontogenetic trajectories from those of *Chromis* sp. The null hypothesis of a common direction of the ontogenetic vectors of the neurocranium cannot be statistically discarded for the comparison of *D. aruanus* with *D. carneus*, and of *D. flavicaudus* with *D. trimaculatus*. For the mandible, it also appears that *D. aruanus*, *D. trimaculatus*, and *D. flavicaudus* have mutually indistinguishable trajectories.

When all species where included in the cross-validation analysis of the regression models, there was clear evidence in favour of the independent trajectory model (superior explanatory power in the cross-validation for 95% of the test data; Table 4) for both the neurocranium and the mandible. When the analysis was restricted to the *Dascyllus* species only, the support for the independent direction model dropped to 95% for the neurocranium, and 87% for the mandible. Pairwise comparisons indicated that *D. aruanus* appeared to have a distinct trajectory in the neurocranium, but typically not in the mandible (although it did appear to differ slightly from *D. carneus*). All other comparisons in the *Dascyllus* failed to reject the null of a shared direction of the trajectory in the cross-validation analysis.

These latter results are reinforced by examination of the deformation grids for largest specimens of each ontogenetic series. Although we have seen some statistical evidence of differences among the ontogenetic trajectories in *Dascyllus* species, the statistical differences appear to be quite small, which raises the issue of how biologically significant these differences are. The differences among *Dascyllus* species in both the ontogenetic angle (Table 3) and the explanatory power of the regression model (Table 4) are lower than between the *Dascyllus* species and the *Chromis* sp. Figures 4 and 5 show that the nature of allometric shape changes in the neurocranium and the mandible is visually very similar within *Dascyllus*. During *Dascyllus* ontogeny, the neurocranium becomes relatively higher and shorter (Fig. 4). This change is mainly related to a heightening of the supraoccipital crest (LM 5-6-7). The prootic (LM 10-11) and the sphenotic (LM 12-13-14-15) are higher at the adult stage. In each *Dascyllus*, the mandible becomes relatively higher during growth (Fig. 5). The dentary shortens and its symphysial part lengthens (LM 1-12). The articulo-angular enlarges and the posterior part of the mandible (retroarticular) extends rostrocaudally (LM 6-7). As seen in Figure 6, the differences among *Dascyllus* in the ontogenetic trajectories at individual landmarks are extremely limited in both skeletal units. For the neurocranium, only slight variations are present in the direction of the heightening of the supraoccipital crest (LM 6).

Comparison of the juvenile and adult shapes among *Dascyllus* sp.

The exploration of shape divergences among *D. aruanus*, *D. carneus*, *D. flavicaudus*, and *D. trimacu-*

Table 4. Results of cross-validation comparison of a regression model with independent trajectories versus a model with a common direction of trajectory, but varying rates along that trajectory

	Neurocranium			Mandible		
	Cross-validation error		Independent model	Cross-validation error		Independent model
Grouping	Independent	Common	Outperforms common	Independent	Common	Outperforms common
All species	0.0629 ± 0.0080	0.1064 ± 0.0280	0.97	0.0963 ± 0.0126	0.1665 ± 0.0126	0.97
Dascyllus only	0.0525 ± 0.0083	0.0806 ± 0.0234	0.95	0.0872 ± 0.0147	0.1250 ± 0.0393	0.87
Pairwise comparisons						
Chromis–D. aru	0.0276 ± 0.0061	0.0687 ± 0.0107	1.00	0.0364 ± 0.00820	0.5359 ± 0.0967	1.00
Chromis–D. car	0.0194 ± 0.0042	0.0848 ± 0.0159	1.00	0.0263 ± 0.0710	0.5511 ± 0.0711	1.00
Chromis–D. fla	0.0232 ± 0.0059	0.1006 ± 0.0150	1.00	0.0309 ± 0.00624	0.4158 ± 0.0378	1.00
Chromis–D. tri	0.0216 ± 0.0037	0.1289 ± 0.0193	1.00	0.0389 ± 0.0094	0.6676 ± 0.1035	1.00
D. aru–D. car	0.0266 ± 0.0055	0.0400 ± 0.0122	1.00	0.0402 ± 0.0091	0.0564 ± 0.0171	0.97
D. aru–D. fla	0.0315 ± 0.0083	0.0461 ± 0.0130	0.95	0.0435 ± 0.0087	0.0619 ± 0.0176	0.93
D. aru–D. tri	0.0307 ± 0.0057	0.0521 ± 0.1430	1.00	0.0513 ± 0.0107	0.0652 ± 0.0196	0.80
D. car–D. fla	0.0241 ± 0.0060	0.0250 ± 0.0045	0.67	0.0345 ± 0.0070	0.0360 ± 0.0087	0.52
D.car–D. tri	0.0217 ± 0.0031	0.0262 ± 0.0075	0.76	0.4300 ± 0.0090	0.0462 ± 0.0103	0.60
D. fla–D. tri	0.0246 ± 0.0056	0.0362 ± 0.0136	0.94	0.0463 ± 0.0112	0.0697 ± 0.0200	0.88

The mean ± SD of the cross-validation error (summed squared residuals) obtained over 100 cross-validation trials is shown. In each cross-validation, 10% of the total data set was used as a test-set, with the remaining 90% formed the training set. Also shown is the fraction of the trials in which the independent trajectory model outperformed the common direction model, by having a lower cross-validation error. For abbreviations of the species, see Table 1.

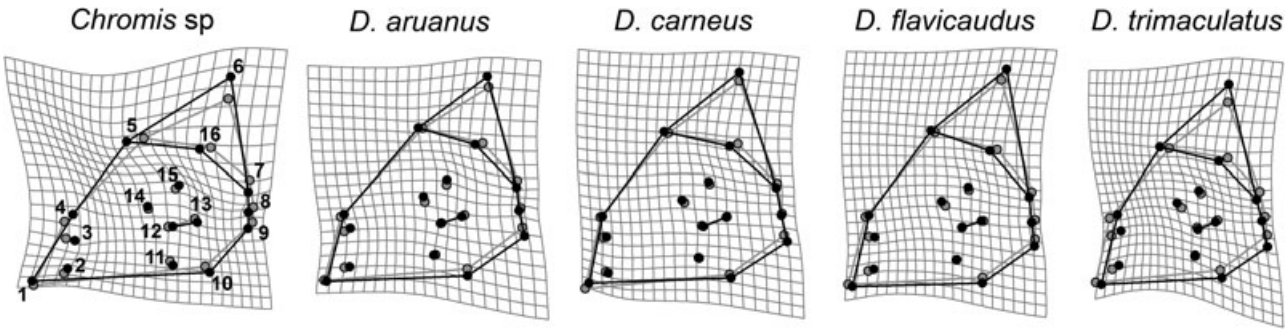

Figure 4. Shapes predicted by the multivariate regression of shape onto size for largest neurocranium of each species sample. The transformations are depicted as deformation grids. Both mean (grey) and adult (black) shapes are shown. The shape difference has been exaggerated for better visualization (×1.6).

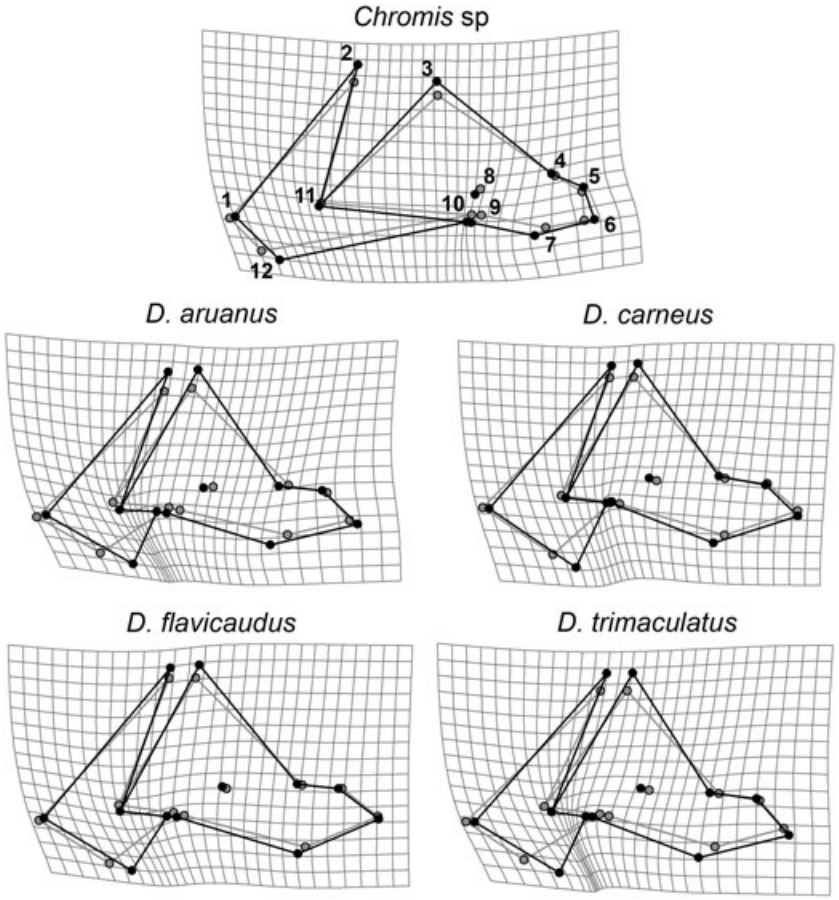

Figure 5. Shapes predicted by the multivariate regression of shape onto size for largest mandible of each species sample. The transformations are depicted as deformation grids. Both mean (grey) and adult (black) shapes are shown. The shape difference has been exaggerated for better visualization (×1.6).

latus at three different sizes along their ontogeny confirms the results of the MANCOVA. Indeed, for both skeletal units, all pairwise *F*-tests among species revealed statistically significant differences in shape at every size ($P = 0.025$). Cross-validation assignment tests on standardized data correctly classified a great proportion of the specimens (< 12% of misclassified specimens in all tests). These CVA assignment rates were slightly greater at the maximum SL than at 20 mm SL in both structures [neurocranium, 94.7%

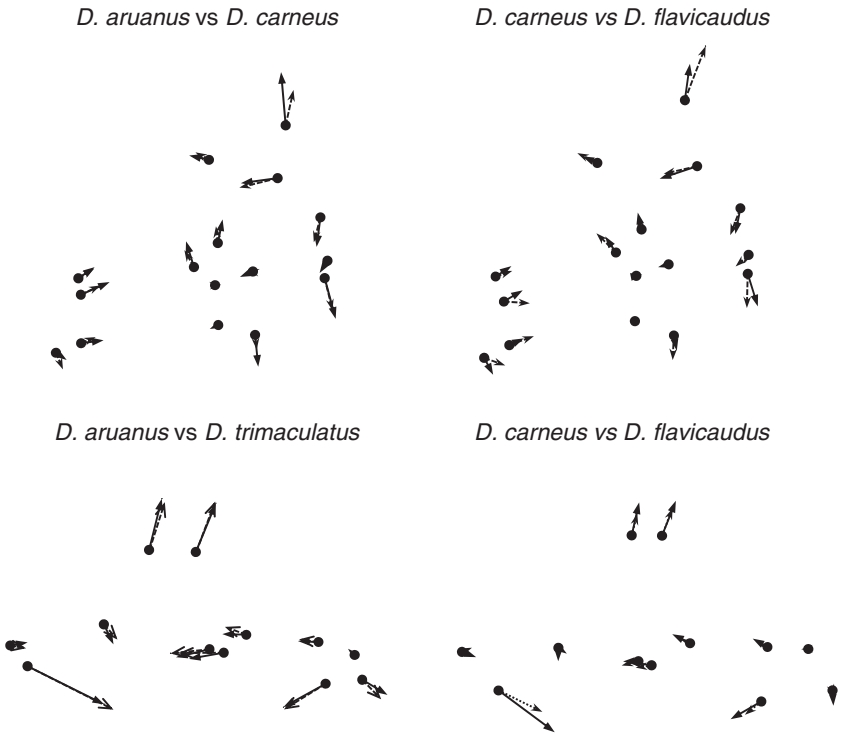

Figure 6. Comparisons of the ontogenetic transformations in neurocranium and mandible shape between some pairs of *Dascyllus* species. The transformations are depicted as vectors of landmark displacements, and are the same changes in shape as shown in the deformation grids in Fig. 5. For each comparison (Sp1 versus Sp2), trajectory of Sp1 is indicated by solid lines, the one of Sp2 by dashed lines.

(20 mm SL) < 96.3% (maximum SL) of correct assignments; mandible, 88.3% (20 mm SL) < 94.4% (maximum SL)]. The shape similarity of the four *Dascyllus* is summarized in Figures 7 and 8 by UPGMA cluster analyses and NMMD plots of the matrix of pairwise PD between species means. In both units, the phenogram and plot topology changes according to the three sizes. The shape similarities among *Dascyllus* change during ontogeny but in opposite ways according to the structure. The dissimilarity in the neurocranium between the small-bodies (*D. aruanus* and *D. carneus*) and the giant (*D. flavicaudus* and *D. trimaculatus*) species increases during the late stage of their ontogeny (Fig. 7). On the other hand, all four species appear to be rather similar based on their mandibular shape at their maximum SL (Fig. 8). At 20 and 60 mm SL, small differences exist in the neurocranium of the *Dascyllus*. These differences were mainly related to the supraoccipital crest (Fig. 7). In Figure 9, CVA shows differences among species at their maximum SL. The giant species clearly showed a relatively shorter and higher neurocranium than the two other species (variations along CV1; Fig. 9). As highlighted by CV2, *D. carneus* slightly differed from the others by a relatively larger front region (LM 4, 5, 14, 15 and 16) (Fig. 9). In the mandible, a 20-mm SL *D. trimaculatus* mainly differed from the other species by having lower coronoid processes (LM 2-3) and a shorter symphysial suture (LM 1-12) (Fig. 8). *Dascyllus aruanus* and *D. carneus* showed the highest mandible with the longest symphysial part of the dentary at 60 mm SL (Fig. 8). At their maximum SL, the CVA showed that the shape differences among *Dascyllus* were not strongly related to body size. Indeed, the small-bodied *D. aruanus* and the large-bodied *D. trimaculatus* showed a total overlap in the shape space defined by CV1 and CV2. Shape variations were mainly related to the dentigerous and the symphisial part of the dentary (CV1 and CV2, Fig. 9).

Comparison of the dynamics of shape change among *Dascyllus* sp.

In both skeletal units, the rate of shape change (Procrustes distance versus ln-CS) significantly differs among *Dascyllus* species (ANCOVA: neurocranium, $F = 4.6479$, d.f. = 3, 180, $P = 0.004$; mandible, $F = 20.883$, d.f. = 3, 188, $P < 0.001$) (Figs 10, 11A). *Dascyllus trimaculatus* showed a higher rate than the two small-bodied species, *D. aruanus* and *D. carneus*, and *D. flavicaudus* for the neurocranium. Conversely,

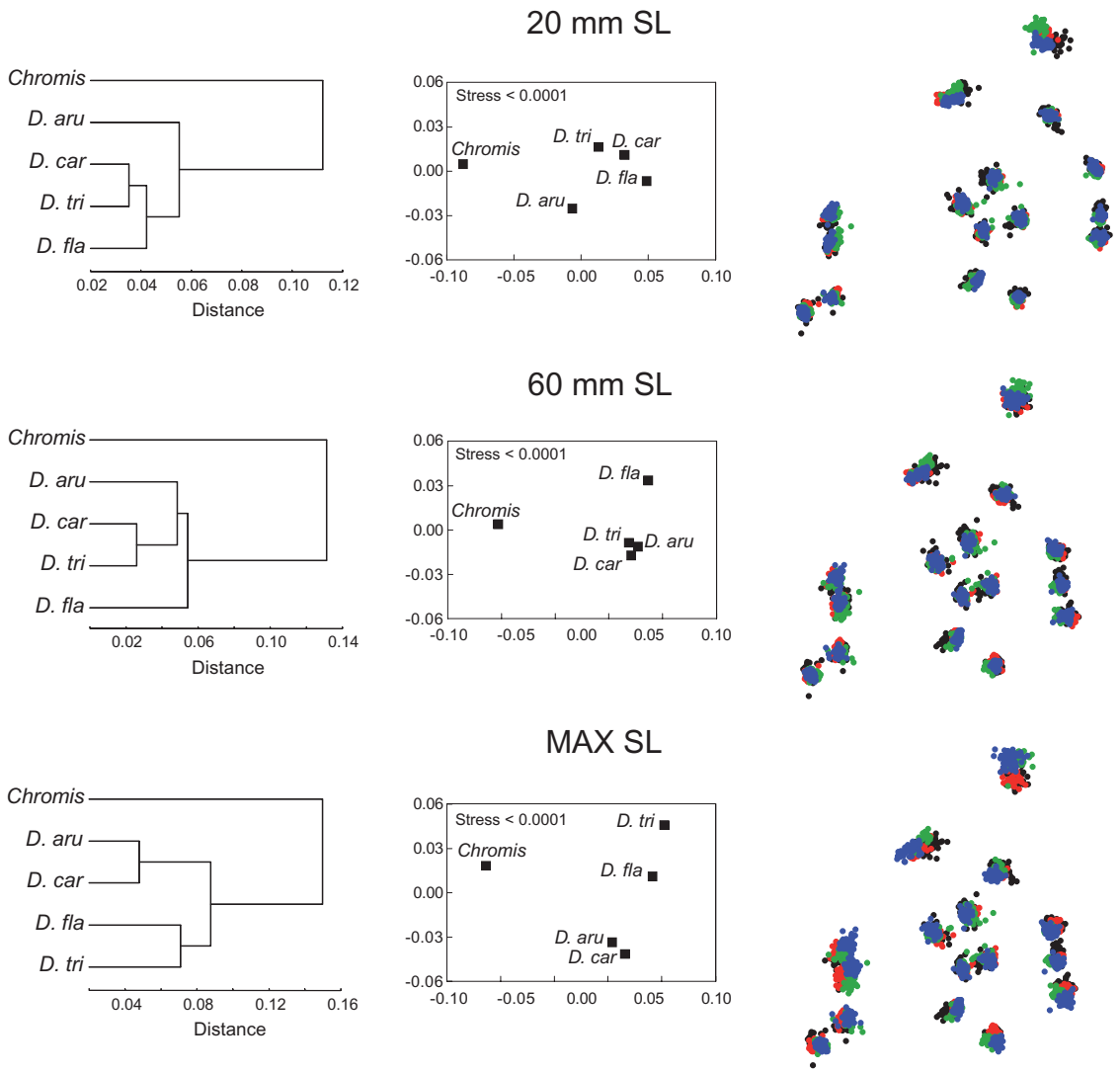

Figure 7. Comparisons of average neurocranium shapes among *Dascyllus aruanus*, *Dascyllus carneus*, *Dascyllus flavicaudus*, and *Dascyllus trimaculatus* at three different stages of their ontogeny: 20 mm standard length (SL), 60 mm SL and their maximum SL. Left: unweighted pair group method with arithmetic mean phenograms based on Procrustes distances between species means. Center: nonmetric multidimensional scaling plots based on Procrustes distances between species means. Right: generalized least squares Procrustes superimposition of the standardized specimens. Black, *D. aruanus*; red, *D. carneus*; green, *D. flavicaudus*; blue, *D. trimaculatus*.

D. aruanus had the highest rate of shape change for the mandible and *D. flavicaudus* had the lowest. The amount of shape change between an average shape at 20 mm SL and at 60 mm SL was almost equal among *Dascyllus* for the neurocranium (Fig. 11B). However, the total length of the ontogenetic trajectory (PDs between an average shapes at 20 mm SL and at the maximum SL) was the highest in *D. trimaculatus* for the neurocranium and the mandible (Fig. 11C). Thus, this species undergoes more shape change in comparison to the other *Dascyllus* studied during the ontogeny. Although the amount of shape change differs significantly (pairwise F-tests, $P = 0.025$) between the small-bodied species (*D. aruanus* and *D. carneus*) for both units, the values remain rather similar compared to those of the two giant species (Fig. 11C). *Dascyllus flavicaudus* had intermediate values based on neurocranial distances (Fig. 11C). Although the rate of shape changes for the mandible is lower in *D. flavicaudus*, it showed a similar length of net ontogenetic trajectory for this structure compared to *D. aruanus* and *D. carneus* as a result of the increased change in CS (i.e. increased ontogenetic duration).

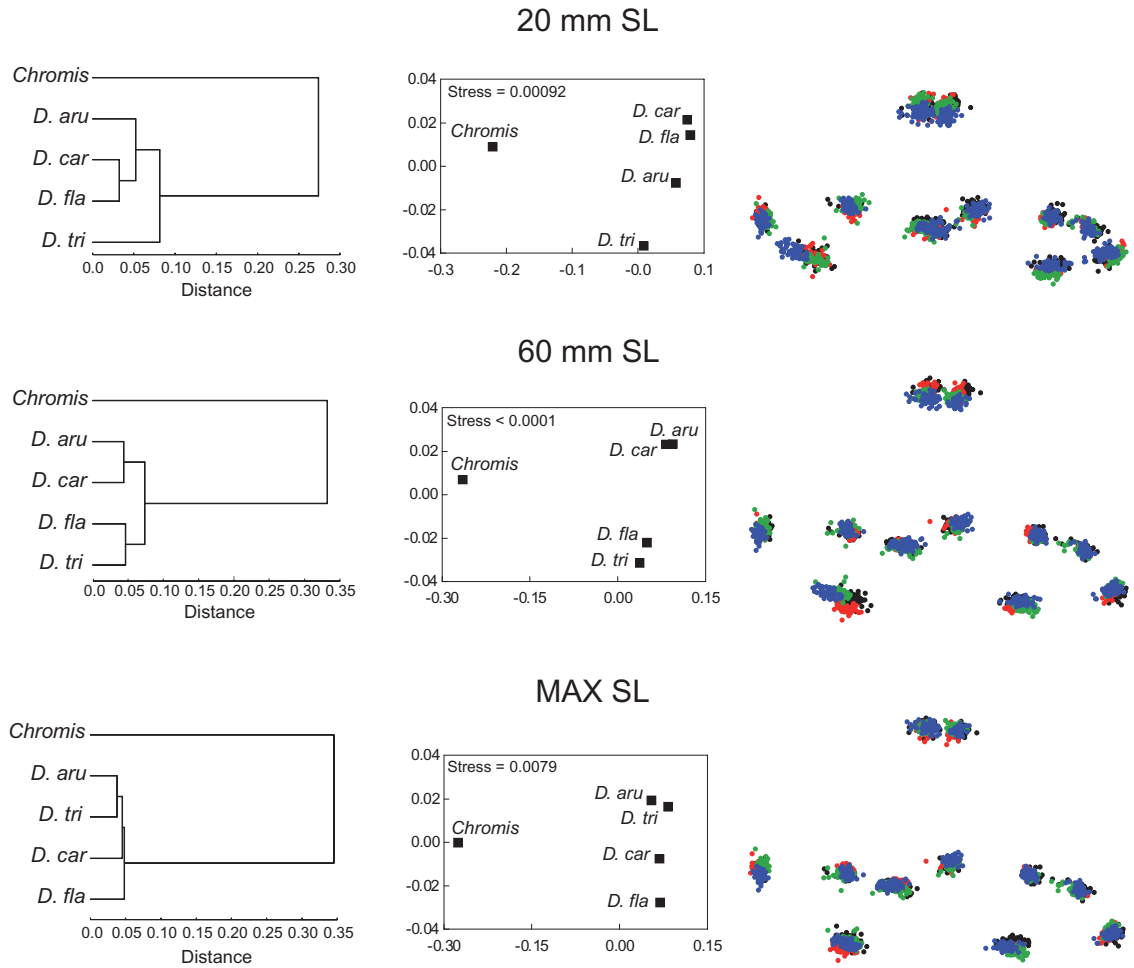

Figure 8. Comparisons of average mandible shapes among *Dascyllus aruanus*, *Dascyllus carneus*, *Dascyllus flavicaudus*, and *Dascyllus trimaculatus* at three different stages of their ontogeny: 20 mm standard length (SL), 60 mm SL and their maximum SL. Left: unweighted pair group method with arithmetic mean phenograms based on Procrustes distances between species means. Center: nonmetric multidimensional scaling plots based on Procrustes distances between species means. Right: generalized least squares Procrustes superimposition of the standardized specimens. Black, *D. aruanus*; red, *D. carneus*; green, *D. flavicaudus*; blue, *D. trimaculatus*.

DISCUSSION

All analyses (PCA, MANCOVA, angles between allometric vectors, cross-validation of regression models) show that the allometric trajectories of all *Dascyllus* are highly divergent from that of *Chromis* sp. Although both genera are grouped in the subfamily Chrominae according to precise morphological traits (e.g. coniform teeth) (Allen, 1991) and molecular data (Quenouille, Bermingham & Planes, 2004; Cooper, Smith & Westneat, 2009), skeletal shape divergences and other morphological differences between some species of each genus have been documented in functional and ecomorphological contexts (Gluckmann & Vandewalle, 1998; Frédérich, Parmentier & Vandewalle, 2006; Frédérich *et al.*, 2008a). The divergence of allometries should clearly contribute to the differentiation of the two genera. We return now to the five questions posed at the start of the study.

ALLOMETRIC TRAJECTORIES WITHIN THE GENUS *DASCYLLUS*

Descriptions of heterochronic processes imply the knowledge of the relations between size, shape, and age (Klingenberg, 1998; Webster & Zelditch, 2005). In the present study, we have no information on chronological age, although size may be viewed as a reasonable proxy of developmental age knowing that the sexual maturity is strongly size related in *Dascyllus* species (Booth, 1995; Asoh, 2003, 2004, 2005). In the

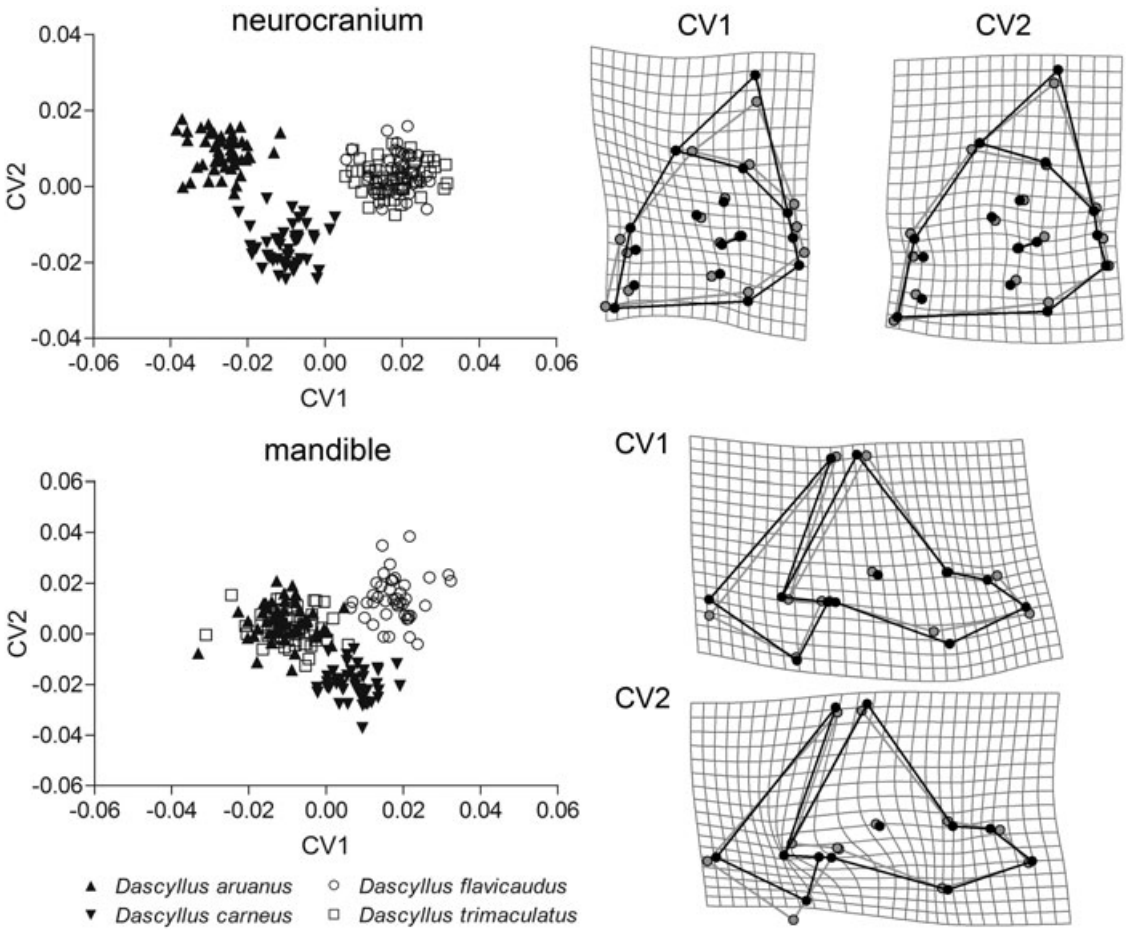

Figure 9. Canonical variate analysis of variation among *Dascyllus aruanus*, *Dascyllus carneus*, *Dascyllus flavicaudus*, and *Dascyllus trimaculatus* for the neurocranium and the mandible. Data are from ontogenetic series and are standardized; comparisons are made at the maximum standard length of each species. The deformation grids show the shape variation calculated by regression on CV axes.

framework of heterochrony, the different patterns of ontogenetic allometry and the shape differences at common size permit the rejection of 'pure' proportioned giantism or hypermorphosis (peramorphism) as the pattern by which the large-bodied *Dascyllus* evolved from the small-bodied ones. The case of the giant *Dascyllus* appears to differ from the ontogenetic scaling revealed in giant transgenic mice using another morphometric method (Shea *et al.*, 1990; Corner & Shea, 1995). However, this comparison has to be made cautiously knowing that the methodological difference (landmark-based geometric morphometric methods versus finite-element scaling method) may induce bias in biological conclusions (Webster & Zelditch, 2005).

The exploration of the ontogenetic trajectories in the Procrustes form space, the test for homogeneity of intercepts, the analysis of the angles between multivariate regression vectors, the cross-validation results based on the regression models and the observations of deformation grids predicted by allometric trajectories all show that the dissociations between *D. aruanus*, *D. carneus*, *D. flavicaudus*, and *D. trimaculatus* may be reasonably described as arising from a series of lateral transpositions of log-linear trajectories. The ontogenetic trajectories of each species are approximately parallel in the 'size-shape' space, as demonstrated by the repeated failure of several tests to reject a null model of a common direction of the ontogenetic trajectories, with the possible exception of *D. aruanus*. Although there is some evidence that the ontogenetic trajectory in *D. aruanus* may differ from the other *Dascyllus* species, visual inspection of the regression plots indicates that this difference does not rise to the same level of biological differences as seen between the *Dascyllus* and *Chromis* sp. It is also clear that a stronger approach to testing the hypothesis of a common trajectory, namely one that could reject a

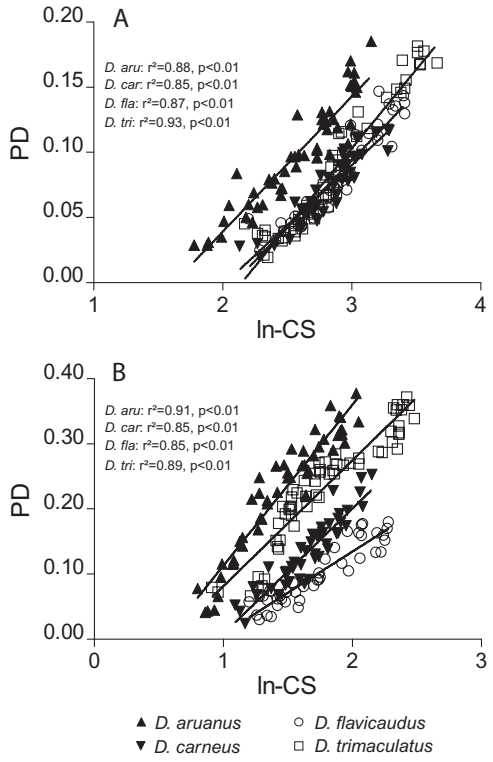

Figure 10. Plots of Procrustes distance between each specimen and the shape of the four smallest specimens on log-transformed centroid size (ln-CS) in the four *Dascyllus* species for the neurocranium (A) and the mandible (B). The R^2 and *P*-value for each linear model is given.

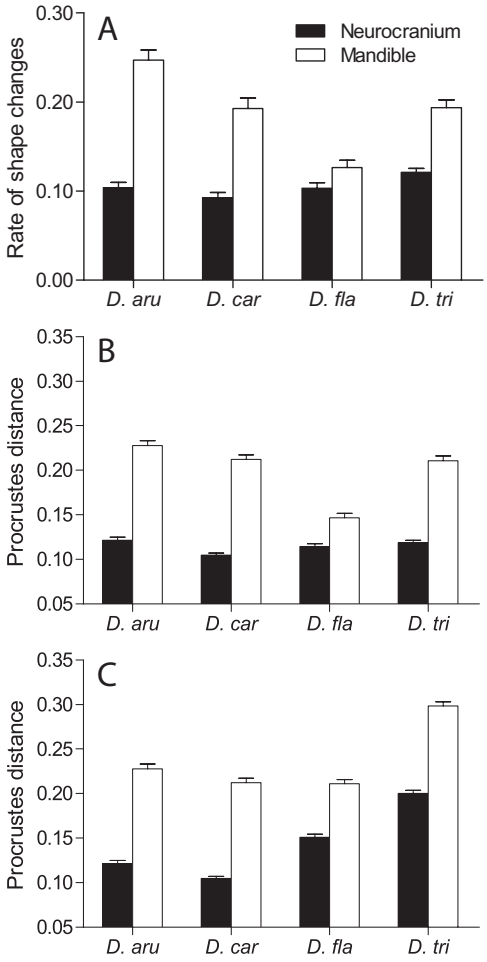

Figure 11. Rate of shape change (A) estimated by the slope of the regression between Procrustes distance and log-values of centroid size for both skeletal units; lengths of ontogenetic trajectories in units of Procrustes distance (B) between mean shapes at 20 mm and at 60 mm standard length (SL) and (C) between mean shapes at 20 mm and at maximum SL for both structures. The error bars indicate the standard error.

hypothesis of differing ontogenetic trajectories in favour of a simple model of shared directions with varying rates, would be very valuable in ontogenetic studies. Similarly, statistically powerful methods to compare the effectiveness of log-linear models of trajectories to more complex polynomial functions of log size should also prove valuable. Although a log-linear model of the mandibular trajectories appears justified in this case, given that at most 1.3% of total variance lies along the curved portion of the trajectory, the ability to effectively compare different multivariate models of ontogenetic trajectories at reasonable sample size would be a major step forward. The use of Procrustes-distance based statistics and permutation methods have proven to be powerful and effective, although there is currently no available model choice procedure other than cross-validation available that utilizes Procrustes distances.

Divergence in shapes between the small-bodied and the giant *Dascyllus*

The analyses of neurocranium and mandible shape divergences at their respective maximum SL permit the rejection of proportioned giantism as the pattern by which giant species evolved from the small ones. Indeed, the neurocranium of the large-bodied species is relatively shorter and has a higher supraoccipital crest than the small ones (Fig. 9). These shape differences at their maximum SL results especially from a lengthening of the ontogenetic trajectories in the giant species. On the other hand, the divergences in mandible shapes are lower between the small-bodied and the giant *Dascyllus* species. Although statistical analysis revealed significant differences, the shape divergences among species at their respective maximum size are more limited and appear not to be related to the 'giant' trait. The data obtained in the present study suggest the evolution of the allometric

patterns of the neurocranium and the mandible shaping large-bodied *Dascyllus* are not totally correlated, but may make sense in a functional context. A relatively common mandible shape between each *Dascyllus* is probably related to their diet, which is essentially composed of planktonic copepods in all species (Randall & Allen, 1977), whereas the neurocranium is a structural unit with more diverse functions, being shaped by eye size and brain structure. Its form is also related to feeding (Liem, 1993; Herrel *et al.*, 2005) and swimming (Videler, 1993) performances. Thus, these different demands taken as a whole lead to shaped variation in the neurocranium of giant and small-bodied species. Interestingly, these differences of shape variation detected in the neurocranium and the mandible are suggestive of functional modularity (Klingenberg, 2008). Indeed, the two skeletal units correspond to relatively independent morphological modules.

Variation of the allometric models among *Dascyllus* sp.

In the case of the genus *Dascyllus*, allometric variation linked to the diversification of the family Pomacentridae is highlighted. Indeed, a comparison of allometric trajectories of the same structures between *D. aruanus* and *Pomacentrus pavo* revealed that the divergences in the neurocranium and the mandible shape result from allometric repatterning (Frédérich *et al.*, 2008b). Lateral transposition indicates a dissociation between species in an earlier period (e.g. during the larval stage) but, during the studied part of their ontogeny, each species of *Dascyllus* shares common trajectories of ontogenetic shape changes (with the possible exception of *D. aruanus*, if the statistical differences observed are truly biologically meaningful). Consequently, the mode of evolutionary modification in *Dascyllus* species of morphological ontogeny may be classified as a case of heterochrony according to the definition of Webster & Zelditch (2005). These results could be linked to a high phylogenetic and/or an ecomorphological signals. Being phylogenetically closely related, the genetic developmental pathways should be conserved in the taxon. Moreover, all *Dascyllus* have a similar diet and share a similar habitat during a part of their ontogeny (Randall & Allen, 1977; Coates, 1980; Mann & Sancho, 2007). Generally speaking, when species are more distant in an evolutionary relationship, it is more probable to see directional change in their allometric trajectories (Weston, 2003). A common trajectory of ontogenetic shape changes shared by two (or more) species of the same genus, as in *Dascyllus* species, is a rather novel result. Cunha *et al.* (2009) recently highlighted that variation in body size among biotypes of the *Squalius alburnoides* complex is the result of ontogenetic scaling. Bastir *et al.* (2007) also addressed the discussion of ontogenetic scaling versus lateral transposition in the context of higher vertebrate evolution. In closely-related species such as humans and Neanderthals, lateral transposition is found rather than truncation or extension of common ontogenetic trajectories (Bastir *et al.*, 2007). Conversely, studies in the trilobite *Nephrolenellus* (Webster *et al.*, 2001; Webster, 2007), in the piranhas *Serrasalmus* (Zelditch *et al.*, 2003), in *Triturus* species (Ivanović *et al.*, 2007), in *Marmota* species (Cardini & O'Higgins, 2005), and in the chimpanzees *Pan* (Mitteroecker *et al.*, 2005) showed directional change in allometric trajectories (i.e. allometric repatterning, Webster & Zelditch, 2005).

The dynamics of shape change differ within the large-bodied species as well as between the large-bodied species and the small ones. Such variation in rate modification being referred as rate heterochrony (Webster & Zelditch, 2005). For the neurocranium, the rate of change in shape seems positively correlated to the maximum adult body size: the largest species (*D. trimaculatus*) has the highest rate of shape change and the smallest have the lowest value (Fig. 11A). This relationship is not observed for the mandible and such a difference between the two structures is difficult to interpret.

Variation of the amount of shape changes among *Dascyllus* sp.

The test for homogeneity of intercepts and the analysis of standardized data allow detections of shape differences among all *Dascyllus* along their whole ontogeny. However, some of these divergences are limited and may not be significant in biological point of view, especially between the two small-bodied species. For example, the length of the ontogenetic trajectories in *D. aruanus* and *D. carneus* are very similar and the differences could be considered as negligible in the present study. On the other hand, the differences in the allometric models between small-bodied and giant species are statistically significant and appear to be of greater biological significance. The length of the ontogenetic trajectories and the distances between the parallel trajectories (i.e. the amplitude of lateral transposition) vary between the small-bodied and the giant species. Additionally, the type of lateral transposition (i.e. event heterochrony according to Webster & Zelditch, 2005) differs according to the skeletal unit and the giant species. Having a higher supraoccipital crest at 20 mm SL, *D. flavicaudus* is closer to its adult shape compared to the situation existing in the others (Fig. 7) and this case may be considered as a predisplacement in the

formalism of Alberch *et al.* (1979). Conversely, *D. trimaculatus* shows a mandible shape that is more distant from the adult one relative to the three other species at 20 mm SL (Fig. 8). This last case may be regarded as a postdisplacement event.

Differences in the evolution of ontogenetic allometries in giant *Dascyllus* species

The two giant species, *D. flavicaudus* and *D. trimaculatus*, have evolved through different allometric mechanisms. These species belong to different lineages and the divergences of developmental parameters agree with phylogenetic data. The rate of shape change differs between the two species. Similarly, the type of lateral transposition varies between *D. flavicaudus* (i.e. predisplacement for the neurocranium) and *D. trimaculatus* (i.e. postdisplacement for the mandibule), showing variation in the timing of development. The types of event heterochrony are not identical for both structures in each species, raising questions about the context of morphological integration (Klingenberg, 2008). Indeed, why does the predisplacement event only concern the neurocranium and not both the neurocranium and the mandible in *D. flavicaudus*? Furthermore, why does the postdisplacement event only concern the mandible and not both the neurocranium and the mandible in *D. trimaculatus*? Differences in life-history between the two giant species cannot explain such modular development, but various genetic or developmental factors probably underlie these different allometric mechanisms and modular patterns. In conclusion, the example of *Dascyllus* demonstrates that giant species may appear during the evolution of a clade by varied alterations of the ancestor allometric model.

The present study details the variation in allometric patterns shaping giant species of fishes. Examples in other animal taxa are required to either confirm our observations or to highlight new patterns of variation, and stronger statistical approaches based on hypothesis testing or model selection would be invaluable to confirm that species share common directions of ontogenetic trajectories. The results obtained in the present study do demonstrate that giant species in a same lineage may evolve by a variety of allometric variations, indicating several distinct pathways to giant forms.

ACKNOWLEDGEMENTS

We would like to thank Y. Chancerelle, P. Ung (CRIOBE, Moorea, French Polynesia), and J. M. Ouin (Aqua-Laboratory, Institut Halieutique et des Sciences Marines, Toliara, Madagascar) for providing hospitality and laboratory facilities, and for helping to collect the fishes. We thank M. Sabaj (ANSP), J. Williams (NMNH), and G. Duhamel (MNHN) for kindly providing a part of the specimens examined in this study. We are also pleased to acknowledge A. Cardini, P. Vandewalle, M. Webster, and two anonymous reviewers for their useful remarks and comments made when reviewing this manuscript. This research received financial support from La Communauté Française de Belgique (Concours des bourses de voyage 2007) and from The Belgian National Fund for Scientific Research (FRS-FNRS) (FRFC contract no. 2.4.583.05).

REFERENCES

Adams DC, Rohlf FJ, Slice DE. 2004. Geometric morphometrics: ten years of progress following the 'revolution'. *Italian Journal of Zoology* **71:** 5–16.

Alberch P, Gould SJ, Oster GF, Wake DB. 1979. Size and shape in ontogeny and phylogeny. *Paleobiology* **5:** 296–317.

Allen GR. 1991. *Damselfishes of the world*. Melle: Publication of natural history and pets book, Mergus.

Angielczyk KD, Sheets HD. 2007. Investigation of simulated tectonic deformation in fossils using geometric morphometrics. *Paleobiology* **33:** 125–148.

Asoh K. 2003. Gonadal development and infrequent sex change in a population of the humbug damselfish, *Dascyllus aruanus* in continuous coral-cover habitat. *Marine Biology* **142:** 1207–1218.

Asoh K. 2004. Gonadal development in the coral reef damselfish *Dascyllus flavicaudus* from Moorea, French Polynesia. *Marine Biology* **146:** 167–179.

Asoh K. 2005. Gonadal development and diandric protogyny in two populations of *Dascyllus reticulatus* from Madang, Papua New Guinea. *Journal of Fish Biology* **66:** 1127–1148.

Bastir M, O'Higgins P, Rosas A. 2007. Facial ontogeny in Neanderthals and modern humans. *Proceedings of the Royal Society of London Series B, Biological Sciences* **274:** 1125–1132.

Bastir M, Rosas A. 2004. Facial heights: evolutionary relevance of postnatal ontogeny for facial orientation and skull morphology in humans and chimpanzees. *Journal of Human Evolution* **47:** 359–381.

Benton MJ. 2002. Cope's rule. In: Pagel M, ed. *Encyclopedia of evolution*. New York, NY: University Press, 185–186.

Bernardi G, Crane NL. 1999. Molecular phylogeny of the humbug damselfishes inferred from mtDNA sequences. *Journal of Fish Biology* **54:** 1210–1217.

Bookstein FL. 1991. *Morphometric tools for landmark data – geometry and biology*. Cambridge: University Press.

Bookstein FL. 1996. Combining the tools of geometric morphometrics. In: Marcus LF, Corti M, Loy A, Naylor G, Slice D, eds. *Advances in morphometrics*. New York, NY: Plenum Press, 131–151.

Booth DJ. 1995. Juvenile groups in a coral-reef damselfish – density-dependent effects on individual fitness and population demography. *Ecology* **76:** 91–106.

Cardini A, O'Higgins P. 2005. Post-natal ontogeny of the mandible and ventral cranium in *Marmota* species (Rodentia, Sciuridae): allometry and phylogeny. *Zoomorphology* **124:** 189–203.

Cheverud JM, Lewis JL, Bachrach W, Lew WD. 1983. The measurement of form and variation in form: an application of three-dimensional quantitative morphology by finite-element methods. *American Journal of Physical Anthropology* **56:** 157–167.

Coates D. 1980. Prey-size intake in humbug damselfish, *Dascyllus aruanus* (Pisces, Pomacentridae) living within social groups. *Journal of Animal Ecology* **49:** 335–340.

Cooper WJ, Smith LL, Westneat MW. 2009. Exploring the radiation of a diverse reef fish family: Phylogenetics of the damselfishes (Pomacentridae), with new classifications based on molecular analyses of all genera. *Molecular Phylogenetics and Evolution* **52:** 1–16.

Corner BD, Shea BT. 1995. Growth allometry of the mandibles of giant transgenic mice: an analysis based on the finite-element scaling method. *Journal of Craniofacial Genetics and Developmental Biology* **15:** 125–139.

Cunha C, Bastir M, Coelho MM, Doadrio I. 2009. Body shape evolution among ploidy levels of the *Squalius alburnoides* hybrid complex (Teleostei, Cyprinidae). *Journal of Evolutionary Biology* **22:** 718–728.

Darlington RB, Smulders TV. 2001. Problems with residual analysis. *Animal Behavior* **62:** 599–602.

Forsman A, Lindell LE. 1993. The advantage of a big head: swallowing performance in adders, *Vipera berus*. *Functional Ecology* **7:** 183–189.

Frédérich B, Pilet A, Parmentier E, Vandewalle P. 2008a. Comparative trophic morphology in eight species of damselfishes (Pomacentridae). *Journal of Morphology* **269:** 175–188.

Frédérich B, Adriaens D, Vandewalle P. 2008b. Ontogenetic shape changes in Pomacentridae (Teleostei, Perciformes) and their relationships with feeding strategies: a geometric morphometric approach. *Biological Journal of the Linnean Society* **95:** 92–105.

Frédérich B, Parmentier E, Vandewalle P. 2006. A preliminary study of development of the buccal apparatus in Pomacentridae (Teleostei, Perciformes). *Animal Biology* **56:** 351–372.

Froukh T, Kochzius M. 2008. Species boundaries and evolutionary lineages in the blue green damselfishes *Chromis viridis* and *Chromis atripectoralis* (Pomacentridae). *Journal of Fish Biology* **72:** 451–457.

Gluckmann I, Vandewalle P. 1998. Morphofunctional analysis of the feeding apparatus in four Pomacentridae species: *Dascyllus aruanus*, *Chromis retrofasciata*, *Chrysiptera biocellata* and *C. unimaculata*. *Italian Journal of Zoology* **65:** 421–424.

Godwin J. 1995. Phylogenetic and habitat influences on mating system structure in the humbug damselfishes (*Dascyllus*, Pomacentridae). *Bulletin of Marine Science* **57:** 637–652.

Herrel A, Van Wassenbergh S, Wouters S, Adriaens D, Aerts P. 2005. A functional morphological approach to the scaling of the feeding system in the African catfish, *Clarias gariepinus*. *Journal of Experimental Biology* **208:** 2091–2102.

Hone DWE, Benton MJ. 2005. The evolution of large size: how does Cope's Rule work? *Trends in Ecology and Evolution* **20:** 4–6.

Hone DWE, Dyke GJ, Haden M, Benton MJ. 2008. Body size evolution in Mesozoic birds. *Journal of Evolutionary Biology* **21:** 618–624.

Hunda BR, Hughes NC. 2007. Evaluating paedomorphic heterochrony in trilobites: the case of the diminutive trilobite Flexicalymene retrorsa minuens from the Cincinnatian series (Upper Ordovician), Cincinnati region. *Evolution & Development* **9:** 483–498.

Ivanović A, Vukov TD, Džukić G, Tomasević N, Kalezić ML. 2007. Ontogeny of skull size and shape changes within a framework of biphasic lifestyle: a case study in six *Triturus* species (Amphibia, Salamandridae). *Zoomorphology* **126:** 173–183.

Klingenberg CP. 1998. Heterochrony and allometry: the analysis of evolutionary change in ontogeny. *Biological Review* **73:** 79–123.

Klingenberg CP. 2008. Morphological Integration and Developmental Modularity. *Annual Review of Ecology, Evolution and Systematics* **39:** 115–132.

LaBarbera M. 1989. Analyzing body size as a factor in ecology and evolution. *Annual Review of Ecology and Systematics* **20:** 97–117.

Liem KF. 1993. Ecomorphology of the Teleostean skull. In: Hanken J, Hall BK, eds. *The skull, vol. 3, functional and evolutionary mechanisms.* Chicago, IL: The University of Chicago Press, 423–452.

Mann DA, Sancho G. 2007. Feeding ecology of the domino damselfish, *Dascyllus albisella*. *Copeia* **3:** 566–576.

Marroig G. 2007. When size makes a difference: allometry, life-history and morphological evolution of capuchins (*Cebus*) and squirrels (*Saimiri*) monkeys (Cebinae, Platyrrhini). *BMC Evolutionary Biology* **7:** 20.

McCafferty S, Bermingham E, Quenouille B, Planes S, Hoelzer G, Asoh K. 2002. Historical biogeography and molecular systematics of the Indo-Pacific genus *Dascyllus* (Teleostei: Pomacentridae). *Molecular Ecology* **11:** 1377–1392.

Mitteroecker P, Gunz P, Bernarhd M, Schaefer K, Bookstein FL. 2004. Comparison of cranial ontogenetic trajectories among great apes and humans. *Journal of Human Evolution* **46:** 679–698.

Mitteroecker P, Gunz P, Bookstein FL. 2005. Heterochrony and geometric morphometrics: a comparison of cranial growth in *Pan paniscus* versus *Pan troglodytes*. *Evolution and Development* **7:** 244–258.

Monteiro LR. 1999. Multivariate regression models and geometric morphometrics: the search for causal factors in the analysis of shape. *Systematic Biology* **48:** 192–199.

Monteiro LR, Cavalcanti MJ, Sommer HJS III. 1997. Comparative ontogenetic shape changes in the skull of *Caiman* species (Crocodylia, Alligatoridae). *Journal of Morphology* **231:** 53–63.

Press WH, Teukolsky SA, Vetterling WT, Flannery BP. 2007. *Numerical recipes, third edition: the art of scientific computing*. Cambridge: Cambridge University Press.

Quenouille B, Bermingham E, Planes S. 2004. Molecular systematics of the damselfishes (Teleostei: Pomacentridae): Bayesian phylogenetic analyses of mitochondrial and nuclear DNA sequences. *Molecular Phylogenetics and Evolution* **31:** 66–88.

Randall HA, Allen GR. 1977. A revision of the damselfish genus *Dascyllus* (Pomacentridae) with the description of a new species. *Records of The Australian Museum* **31:** 349–385.

Randall JE, Randall HA. 2001. *Dascyllus auripinnis*, a new pomacentrid fish from atolls of the Central Pacific ocean. *Zoological Studies* **40:** 61–67.

Rohlf FJ. 1993. Relative warps analysis and an example of its application to mosquito wings. In: Marcus LF, Bello E, Garcia-Valdecasas A, eds. *Contributions to morphometrics*. Madrid: Monografias del Museo Nacional de Ciencias Naturales, CSIC, 131–159.

Rohlf FJ, Marcus LF. 1993. A revolution in morphometrics. *Trends in Ecology and Evolution* **8:** 129–132.

Rohlf FJ, Slice D. 1990. Extensions of the procrustes method for the optimal superimposition of landmarks. *Systematic Zoology* **39:** 40–59.

Sale P. 1971. Extremely limited home range in a coral reef fish *Dascyllus aruanus*. *Copeia* **2:** 324–327.

Shea BT. 1992. Developmental perspective on size change and allometry in evolution. *Evolutionary Anthropology* **1:** 125–134.

Shea BT, Hammer RE, Brinster RL, Ravosa MR. 1990. Relative growth of the skull and postcranium in giant transgenic mice. *Genetical Research* **56:** 21–34.

Slice D. 1999. *Morpheus et al*. New York: Department of Ecology and Evolution, State University of New York.

Taylor WR, Van Dyke GC. 1985. Revised procedure for staining and clearing small fishes and other vertebrates for bone and cartilage study. *Cybium* **9:** 107–121.

Videler JJ. 1993. *Fish swimming*. London: Chapman & Hall.

Webster M. 2007. Ontogeny and evolution of the early Cambrian trilobite genus *Nephrolenellus* (Olenelloidea). *Journal of Paleontology* **81:** 1168–1193.

Webster M, Sheets HD, Hughes NC. 2001. Allometric patterning in trilobite ontogeny: Testing for heterochrony in Nephrolenellus. In: Zelditch ML, ed. *Beyond heterochrony*. New York, NY: Wiley and Sons, 105–144.

Webster M, Zelditch ML. 2005. Evolutionary modifications of ontogeny: heterochrony and beyond. *Paleobiology* **31:** 354–372.

Weston EM. 2003. Evolution of ontogeny in the hippopotamus skull: using allometry to dissect developmental change. *Biological Journal of the Linnean Society* **80:** 625–638.

Zelditch ML, Sheets HD, Fink WL. 2000. Spatiotemporal reorganization of growth rates in the evolution of ontogeny. *Evolution* **54:** 1363–1371.

Zelditch ML, Sheets HD, Fink WL. 2003. The ontogenetic dynamics of shape disparity. *Paleobiology* **29:** 139–156.

Zelditch ML, Swiderski DL, Sheets HD, Fink WL. 2004. *Geometric morphometrics for biologists: a primer*. San Diego, CA: Elsevier Academic Press.

APPENDIX

Abbreviations: ANSP, Academy of Natural Sciences (Philadelphia, PA, USA); MNHN, Museum National d'Histoire Naturelle (Paris, France); NMNH, National Museum of Natural History (Washington, DC, USA).

Dascyllus carneus ANSP lot 109319 (15 specimens); MNHN, 2005-1974; NMHN, 281395.